Attractive and repulsive tip-sample interaction regimes in tapping-mode atomic force microscopy

Ricardo García* and Alvaro San Paulo
Instituto de Microelectrónica de Madrid, CSIC, Isaac Newton 8, 28760 Tres Cantos, Spain
(Received 12 February 1999)

Attractive and repulsive tip-sample interaction regimes of a force microscope operated with an amplitude modulation feedback were investigated as a function of tip-sample separation, free amplitude, and sample properties. In the attractive regime, a *net attractive force* dominates the amplitude reduction while in the repulsive regime the amplitude reduction is dominated by a *net repulsive force*. The transition between both regimes may be smooth or steplike, depending on free amplitude and sample properties. A steplike discontinuity is always a consequence of the existence of two oscillation states for the same conditions. Stiff materials and small free amplitudes give rise to steplike transitions while the use of large free amplitudes produce smooth transitions. Simulations performed on compliant samples showed cases where the cantilever dynamics is fully controlled by a net attractive force. Phase-shift measurements provide a practical method to determine the operating regime. Finally, we discuss the influence of those regimes in data acquisition and image interpretation. [S0163-1829(99)03231-2]

I. INTRODUCTION

Dynamic atomic force microscopy (AFM) methods offer three main advantages with respect to static (contact) AFM. First, the tip motion is sensitive to both forces and force gradients. Suitable experimental setups may allow simultaneous force and interatomic potential mapping. Second, in contact AFM the tip-sample interaction is measured following the cantilever's deflection. In dynamic AFM the oscillation amplitude, the frequency, and the phase shift, as well as the cantilever deflection, may be recorded. This opens several channels for simultaneous data acquisition, each of them describing a different property. Third, the forces required to obtain a stable signal in contact AFM may involve some sort of sample damage that prevents high-resolution imaging. This applies, in particular, to imaging compliant materials (biomolecules and polymers) in air or semiconductors in ultrahigh vacuum. Dynamic force microscopy methods may substantially reduce the sample damage. The above advantages are being exploited by using different dynamic AFM modes.[1–7]

Tapping-mode AFM is a high-amplitude dynamic mode where an amplitude modulation feedback is used to image the sample topography.[6] The cantilever-tip ensemble is oscillated at a frequency close to its resonance. The sample is imaged while the feedback adjusts the tip-sample separation to keep the oscillation amplitude at a fixed value. This mode has allowed routine high-resolution imaging of a variety of samples, such as DNA-protein complexes,[8] polymers,[9] and nanometer-scale structures.[10]

Earlier works have already established the basic equation that governs the tip motion.[7,11–14] In spite of the very extensive experimental use of the tapping-mode AFM, a detailed understanding of the observed tip's motion as a function of sample properties, tip's geometry, and tip-sample separation is still emerging. This lack of understanding makes it difficult to interpret tapping-mode AFM images in terms of topographic variations.[15]

Initially, it was assumed that at one end of the oscillation the tip established mechanical contact with the sample surface.[6] Repulsive forces were thought to be the main mechanism to control the amplitude, although several experimental[13,16,17] and theoretical[13,18] results pointed out that long-range attractive forces could also contribute to the reduction of the amplitude. The contribution of attractive forces could alter the interpretation of a tapping-mode AFM image; however, their role is still largely neglected. In addition, a scheme to classify the mechanisms of amplitude reduction in tapping mode has not been proposed yet.

In this paper we show that an AFM operated with an amplitude modulation feedback has two regimes of operation, *attractive* and *repulsive*. In the first regime, a net attractive force dominates the amplitude reduction while in the other a net repulsive force controls the cantilever dynamics. The operating regime is attractive when the average force in one oscillation is negative. With this definition both regimes may involve long-range attractive forces as well as short-range repulsive forces. We study how the transition between the attractive and the repulsive regime is reflected in the tapping-mode parameters. We also discuss the influence of those regimes in data acquisition and image interpretation.

In most situations, the amplitude decreases with the tip-sample proximity. However, a sharp jump in the amplitude curves has been reported by experiments and simulations.[13,16] This jump has been attributed to the onset of the repulsive regime, i.e., the oscillation switches from a purely noncontact (long-range attractive forces) to tapping mode (attractive and repulsive). However, we find that a steplike discontinuity in the amplitude curve is not an exclusive characteristic of the noncontact to intermittent contact transition. We show that a discontinuity is always a consequence of the existence of two oscillation states.

The transition between the attractive and repulsive regime may be smooth or steplike, depending on free amplitude and material properties. The combination of stiff materials and small free-oscillation amplitudes usually gives rise to discontinuities. On the other hand, the simulations performed for very compliant samples showed no transitions. The ampli-

tude reduction is solely controlled by the attractive regime.

In Sec. II the details of the model and the computational method are described. The transition between attractive and repulsive regimes is discussed in Sec. III. Amplitude, average force, and contact time dependence on tip-sample separation are used to study the transition. In Sec. IV we study the physical origin of a steplike transition. The bistable response of the cantilever is outlined. In Sec. V we propose phase-shift measurements to determine the operating regime. The influence of the elastic properties on the transition is analyzed in Sec. VI. Finally, in Sec. VII our main findings and their experimental implications are summarized.

II. MODEL

A. Motion equation

The dynamic response of the cantilever-tip ensemble driven by an external and sinusoidal signal has been simulated by different authors.[7,11–14] The dominant contributions considered in the equation of motion of the cantilever are its elastic response, the hydrodynamic damping with the medium, the tip-sample interaction, and the excitation force. The resulting nonlinear, second-order differential equation is as follows:

$$m\frac{dz^2}{d^2t} = -k_c z - \frac{m\omega_0}{Q}\frac{dz}{dt} + F_{1s} + F_0\cos\omega t, \tag{1}$$

where F_0 and ω ($\omega = 2\pi f$) are the amplitude and angular frequency of the driving force, respectively; Q, ω_0, and k_c are the quality factor, angular resonance frequency, and spring constant of the free cantilever, respectively. $F_{\rm ts}$ denotes the tip-sample interaction. The above equation implies several assumptions. (i) It considers the cantilever-tip ensemble as a point-mass spring. (ii) The Q factor used here is independent of tip-sample separation. The first assumption ignores the contribution to the cantilever motion of the higher flexural modes of the lever.[19] The second one neglects changes in the hydrodynamic damping of the cantilever during its motion.[20]

B. Tip-sample interaction

The tip-sample geometry is simulated by a sphere (tip) and a flat (sample). Several studies have shown that this geometry is a reasonable approximation to the tip-sample geometry.[6,21] The tip-sample interaction contains attractive and repulsive forces. Long-range attractive forces are derived from the nonretarded van der Waals energy for two atoms in vacuum. Assuming additivity, for a sphere-flat geometry the van der Waals force is ($d > \mathbf{a}_0$)

$$F_{ts}(z_c,z) = -\frac{HR}{6(z_c+z)^2}, \tag{2}$$

where H is the Hamaker constant and R the tip radius. For convenience, the tip-sample instantaneous separation d is calculated as the sum of the tip-sample rest distance (z_c) and the instantaneous tip position z ($d = z_c + z$). The origin of the z coordinate is the tip's rest position (Fig. 1). a_0 is an intermolecular distance that is introduced to avoid the divergence of Eq. (2) (see Ref. 21). For separations $d < a_0$, the resulting van der Waals force is identified with the adhesion force given by the Dejarguin-Muller-Toporov (DMT) theory,[22,23]

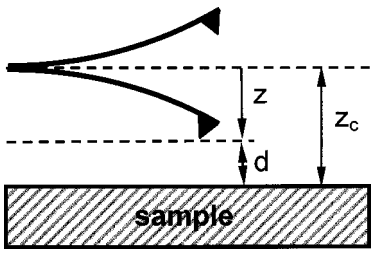

FIG. 1. Scheme of the cantilever-tip and the sample. The average (rest) cantilever position is the origin of the z coordinate. The instantaneous tip-sample separation d is the sum of the rest separation z_c (positive) and z (with its sign).

$$F_a = 4\pi R\gamma = \frac{HR}{6a_0^2}, \tag{3}$$

where γ is the surface energy.

In addition to the adhesion force, during the contact ($d < a_0$) there are repulsive forces arising from Pauli and ionic repulsion. The repulsive force and the sample deformation are modeled by using the DMT contact mechanics,

$$F_{ts}(z_c,z) = -\frac{HR}{6a_0^2} + \frac{4}{3}E^*\sqrt{R}(a_0 - z - z_c)^{3/2} \tag{4}$$

$$\frac{1}{E^*} = \frac{(1-\nu_t^2)}{E_t} + \frac{(1-\nu_s^2)}{E_s}, \tag{5}$$

where E_x and ν_x are the tip (sample) elastic modulus and the Poisson coefficients, respectively.

This model is based on a continuum theory; it may not be suitable to explain some phenomena involving lateral resolutions below 1 nm, where the discrete character of the matter cannot be ignored. However, this limitation does not seem to have many practical consequences. To our best knowledge tapping-mode AFM images cannot claim a lateral resolution of say less than 1–2 nm.

C. Numerical simulations

In the above model the sample is characterized by the Young modulus E, the Hamaker constant H, the surface energy γ, and the Poisson coefficient. The numerical simulations have been performed for silicon dioxide (SiO_2) $E = 70$ GPa, $\gamma = 31$ mJ/m^2, polystyrene $E = 1.2$ GPa, $\gamma = 35$ mJ/m^2, and polyethylene $E = 0.087$ GPa, $\gamma = 32$ mJ/m^2. The Hamaker values are deduced from the Lifshitz theory, $H(SiO_2) = 6.4\times10^{-20}$ J, $H(PS) = 7.1\times10^{-20}$ J, $H(PE) = 6.6\times10^{-20}$ J. A Poisson coefficient of 0.3 has been used for the materials. If we exclude small biomolecules or very thin molecular films, where E may not be well defined, SiO_2 (stiff), PS (*intermediate*), and PE (compliant) can be considered as representatives of the materials currently being studied by tapping-mode AFM. For the cantilever-tip system we have used a radius $R = 20$ nm, $Q = 400$, $f_0 = 350$ kHz, and $k_c = 40$ N/m.

Most of the cantilevers used in tapping-mode AFM are made of silicon with $E \approx 130$ GPa, i.e., several times higher

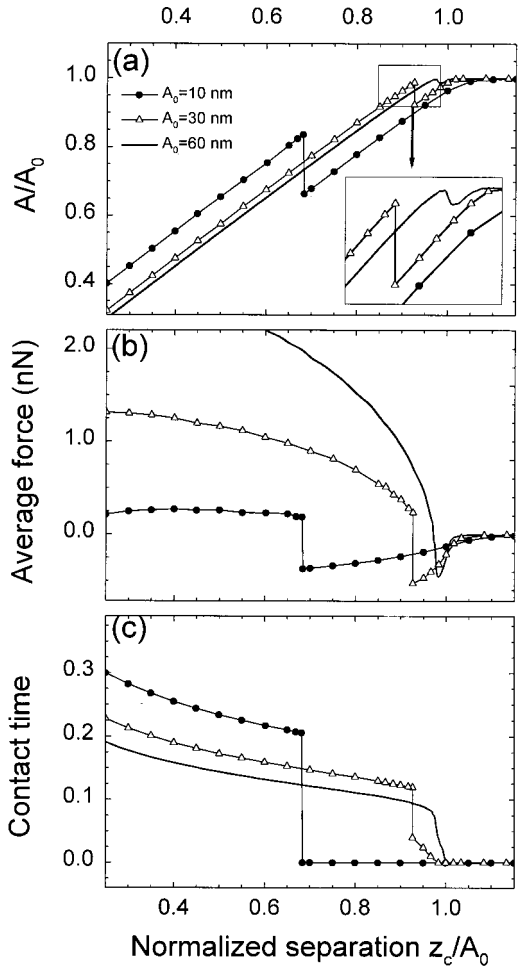

FIG. 2. (a) Amplitude, (b) average force, (c) contact time dependence on tip-sample separation for three free amplitudes. The separation is normalized by taking the ratio z_c/A_0. $E=1.2$ GPa, working frequency, $f_0=350$ kHz.

than the E of the samples simulated here. We will assume that the total tip-sample force is relaxed in the deformation of the sample. The simulations have been performed for $f=f_0$.

A standard fourth-order Runge-Kutta algorithm has been used to solve Eq. (1). For each average tip-sample separation, the conditions used to begin the numerical integration are $z_i=A_{i-1}$ and $dz_i/dt=0$. The phase shift is extracted from the argument of the complex fast Fourier transform of the solution.

III. AMPLITUDE, AVERAGE FORCE, AND CONTACT TIME DEPENDENCE ON TIP-SAMPLE SEPARATION

The oscillation amplitude A is the key experimental parameter measured in tapping-mode AFM. In this section, besides the amplitude we also calculate the average force and the contact time as a function of the tip-sample rest separation z_c for the intermediate material, $E\sim 1$ GPa.

A. Amplitude

Figure 2(a) shows the oscillation amplitude for three different free amplitudes $A_0=10$, 30, and 60 nm (approaching curve). All of them show four different regions as z_c is changed. First, there is a flat region for large z_c. The effect of attractive forces on the oscillation is negligible. Second, at separations slightly larger than A_0, the cantilever starts to sense the long-range attractive force. This usually reduces the amplitude as z_c is reduced. If the working frequency is smaller than the resonance frequency, an initial increase of the amplitude should be expected. This situation is thoroughly discussed by Anczykowski, Krüger, and Fuchs.[13] Third, there is a transition region where the amplitude shows an increase. Fourth, after the transition the amplitude decreases linearly with slope unity.

The shape of the transition curve depends on the free amplitude. For amplitudes 10 and 30 nm a steplike discontinuity is observed while for $A_0=60$ the transition is continuous. The transition is shifted to larger normalized separations (z_c/A_0) when A_0 is increased. It goes from 0.67 (6.7 nm) to 0.97 (58 nm).

In all the cases studied, the amplitude curve by itself does not reveal if its reduction is the result of attractive interactions, repulsive interactions, or a combination of both interactions.

B. Average force

In Fig. 2(b) the average force experienced by the tip during a symmetric cycle is plotted. For $A_0=10$ nm, at large z_c the average force is negative (attractive). It increases in absolute value as z_c decreases until a sudden change of sign is observed. From there on, the average force shows a slight increase until a maximum is found. A similar behavior is observed for $A_0=30$ nm. However, for $A_0=60$ nm the force shows a continuous change with z_c. The average repulsive forces are in the 0.2–2 nN range; however, peak forces of 10–40 nN are found.

The comparison of Figs. 2(a) and 2(b) shows a correspondence between the changes observed in the amplitude and in the force curves. The force curves allow us to define two regimes of operation, attractive and repulsive. The relevant point is that for $A_0=30$ and 60 nm, there are z_c values where the attractive regime also involves short-range repulsive forces. In other words, there is tip-sample intermittent contact in the attractive regime. Simulations performed with compliant materials show better this effect (Sec. VI).

C. Contact time

To further clarify the involvement of short-range repulsive forces in the transition we have calculated the time per oscillation that the tip is in mechanical contact with the sample. This time is known as contact time t_c (Tamayo and Garcia[7]). The contact time is normalized by the period of the oscillation T.

For $A_0=10$ nm, at large separations, long-range attractive forces reduce the oscillation amplitude and $t_c=0$. At some z_c a steplike discontinuous transition between a purely attractive regime $(t_c=0)$ and a repulsive regime $(t_c\neq 0)$ is observed. For $A_0=30$ nm, t_c also shows a steplike discontinuity but this is preceded by a small but continuous change from 0 to 0.02 T. This means that before the jump, the tip is already in intermittent contact with the sample, i.e., under the influence of short-range repulsive forces. For $A_0=60$ nm, the slope of t_c during the transition is high but finite.

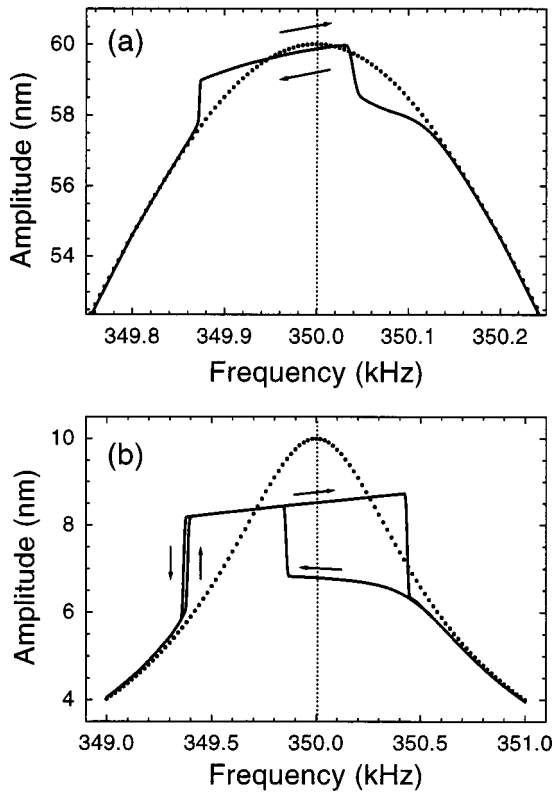

FIG. 3. Frequency response of the cantilever. The amplitude is plotted as a function of the driving frequency. The free oscillating case is plotted by a dotted line. (a) The numerical simulations have been performed for $A_0=60$ nm and $z_c=58.2$ nm and (b) $A_0=10$ nm and $z_c=7$ nm. The arrows indicate the direction of the frequency sweeps. $E=1.2$ GPa and $f_0=350$ kHz.

Once the transition has been completed, i.e., when the net force is positive, t_c grows monotonously with z_c decreasing. For standard working conditions, the contact time represents about 10–30 % of the period of the oscillation.

IV. FREQUENCY RESPONSE OF THE CANTILEVER

In this section we study the physical origin of the steplike discontinuity shown by some of the amplitude, force, or contact time curves. We start with the examination of the frequency response of a vibrating cantilever under nonlinear interactions.

In Fig. 3 the amplitude is plotted as a function of the excitation frequency for two free amplitudes, $A_0=10$ and $A_0=60$ nm. The calculations are performed for the same sample parameters as in Fig. 2. Figure 3(a) shows the results for $A_0=60$ nm and $z_c=58.2$ nm, when the frequency goes from low to high frequencies (upward sweep) or from high to low frequencies (downward sweep). At frequencies far from the free resonance, the behavior is almost harmonic. Then, there is a steep but continuous increase of the amplitude when its value is close to z_c. The simultaneous calculation of the contact time shows that this increase marks a continuous transition from noncontact to intermittent contact. From there on, the amplitude increases until there is a steep but continuous decrease. This continuous decrease marks the transition from intermittent contact to noncontact. The overlap between upward and downward sweeps reflects that for a given set of conditions the equation of motion has a single solution.

When the cantilever is oscillated with a smaller free amplitude $A_0=10$ nm and $z_c=7$ nm a remarkable feature appears [Fig. 3(b)]. For some frequencies, two possible solutions for the amplitude are possible. Starting from low frequencies, the oscillation amplitude remains almost harmonic until a sudden increase of the amplitude is observed. From there on, the amplitude increases linearly until there is a sudden step down. At higher frequencies the oscillation is almost harmonic and the free and perturbed curves overlap.

Now let us examine the curve when the simulations are performed from the right side (downward sweep). Far from resonance, the cantilever oscillates well above the sample. The values of the amplitude match those of the free oscillation and the upward sweep. However, at frequencies closer to the free resonance, attractive forces reduce appreciably the oscillation and the curve departs from both the free and upward sweep. A hysteresis loop appears. At some point, there is a sudden increase of the amplitude. In this case the jump marks the transition from noncontact to intermittent contact. From there on, the upward and downward sweeps overlap until the frequency that marks the intermittent to noncontact transition is reached. Another hysteresis loop is found.

The above results are interpreted as follows. For small free amplitudes and frequencies close to the free resonance, two steady states for the amplitude are possible. A higher amplitude state that implies tip-sample contact and a lower amplitude state, that may or may not imply tip-sample contact [compare curves in Fig. 2(c)]. The jump marks the transition between one state to the other. This is also known as the bistable behavior.[24–26] The system will reach one state or the other, depending on the starting conditions (for example, upward vs downward sweeps). The bistability depends on the sample properties (interaction surface potential), free amplitude, tip-sample distance, and working frequency. From the above results and those presented below (Sec. VI) it is deduced that the combination of stiff materials and relatively small amplitudes set the conditions to observe steplike discontinuities. The reasoning also implies that the above discontinuities have a very different physical origin from the jump-to-contact often described in AFM.

V. PHASE-SHIFT DETERMINATION OF THE TIP-SAMPLE INTERACTION REGIME

To use amplitude curves to determine experimentally the operating regime may be time consuming or impractical. The contact time cannot be directly measured and average force measurements are still being developed.[27] In this section we show that the phase shift that exists between the driving force and the cantilever response allows us to identify whether the operating regime is attractive or repulsive. In the calculations we have taken the standard convention[28] that at resonance a forced harmonic oscillator has a phase lag of 90° with respect to the driving force. The model used only takes into account phase shifts due to elastic interactions. For a discussion about elastic and inelastic contributions to the phase shift in tapping mode see Refs. 29 and 30.

Figure 4 shows the phase shift curves for three free am-

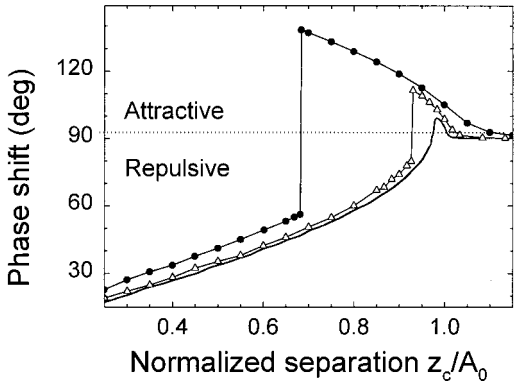

FIG. 4. Phase-shift dependence on tip-sample separation. The separation is normalized by taking the ratio z_c/A_0. Symbols and parameters are as in Fig. 2.

plitudes, 10, 30, and 60 nm [see also Fig. 2(b)]. At large separations, the force and their gradient is negligibly small, Φ remains constant and equal to 90°. At some separation, Φ grows continuously as z_c is decreased. This change in Φ matches the increase (magnitude) observed in the attractive force. When the force changes sign abruptly ($A_0=10$ and 30 nm) Φ also shows a discontinuous change from values above 90° to values below 90°. When the force becomes more repulsive, Φ becomes smaller. For $A_0=60$ nm, Φ changes continuously from values above 90° to values below 90°. The phase always follows the changes observed in the average force.

A practical experimental rule can be deduced. The attractive regime is characterized by phase shifts $\Phi>90°$ while in the repulsive regime Φ is always below 90°.

VI. MATERIAL PROPERTIES INFLUENCE ON THE ATTRACTIVE-REPULSIVE TRANSITION

The conclusions of the preceding sections are general; however, the presence or not of the attractive-repulsive transition for a given amplitude also depends on the material properties. In Fig. 5 is presented a normalized plot that reflects the relative contribution of the attractive regime as a function of the free amplitude for a stiff, intermediate, and compliant material, respectively. The relative contribution of the attractive regime is calculated by taking the ratio between

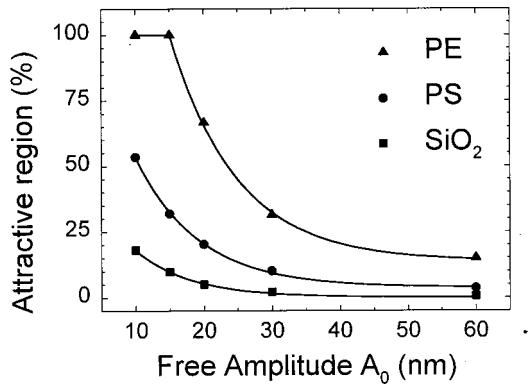

FIG. 5. Map of the attractive regime for different materials (compliant, intermediate, and stiff) and free amplitudes.

the interval of z_c values where the amplitude is decreased by a net attractive force and A_0. To get this figure, for each free amplitude and material the corresponding amplitude vs the z_c curve was calculated. A ratio different from zero means that there is an interval of set point amplitudes where the dynamic force operation is stable in the attractive regime.

The contribution of attractive forces to the amplitude reduction is more noticeable for small free amplitudes. However, sample properties also play a role. The interval of tip-sample separations where the amplitude reduction is controlled by the attractive regime can be quite small for a stiff material and a large free amplitude. For example, SiO_2 shows this behavior when A_0 is in the 30 to 60 nm range. The opposite case happens for a very compliant material. There, the amplitude reduction can be totally dominated by attractive forces. For example, the simulation for PE shows no repulsive regime for A_0 smaller than 15 nm.

VII. DISCUSSION AND CONCLUSIONS

We have presented a detailed study of the behavior of a force microscope operated with an amplitude modulation feedback, what usually is known as the tapping-mode operation. Our results may be summarized in three points. First, an amplitude modulation feedback has two regimes of operation, attractive and repulsive. Phase-shift measurements provide an immediate determination of the operating regime. Second, the transition between attractive and repulsive regimes may be abrupt or smooth depending on the free amplitude and sample properties. Third, the presence of an abrupt change in the amplitude or the force is attributed to the existence of two oscillation states for the same operating conditions.

In the attractive regime the average force per cycle is negative. In general, this regime involves long-range attractive and short-range repulsive forces. However, the sample properties allow some classification. Stiff samples and relatively small amplitudes 10–30 nm usually define an interval of z_c where the attractive regime is dominated exclusively by long-range attractive forces (noncontact). The tip-sample interaction potential for a stiff sample has a very high slope, as a consequence even very small contact times produce large repulsive forces. This gives rise to a net positive force. This effect precludes the existence of an attractive regime involving intermittent contact.

On the other hand, an attractive regime that involves long-range attractive forces and short-range repulsive forces is characteristic of compliant or very compliant materials. Those samples may experience large deformations under tip-sample contact. As a consequence, the net value of the force may be negative although there is tip-sample intermittent contact.

The identification of the operating regime is critical to imaging heterogeneous samples with different elastic and/or adhesion properties. The operating regime could change from region to region of the sample due to differences in elasticity. To keep the set point amplitude fixed, the feedback could interpret this change as a topographic variation. This would introduce features in the image unrelated to the *true* topography of the sample. Phase-shift measurements provide a practical and unambiguous method to identify the operat-

ing regime. Conditions that imply phase shifts above 90° are characteristic of an attractive regime while conditions that set phase shifts below 90° are characteristic of a repulsive regime.

The presence of a steplike discontinuous transition in amplitude curves, however, is not solely a feature of a noncontact to intermittent contact transition. It can also be observed between two oscillations that involve intermittent contact [see $A_0 = 30$ nm in Fig. 2(c)]. The discontinuity is always associated with the existence, for a given A_0, z_c, E, and working frequency of two stable oscillation states. The step represents the transition between those states. It also underlines the nonlinear character of the tip-sample interaction potential. On the other hand, a smooth transition is a consequence of the existence of a single oscillation state.

A sharp, discontinuous transition between the attractive and the repulsive regime may be expected for small free amplitudes and stiff materials. The first requirement is needed in order to have both regimes. The second requirement sets the nonlinear interaction potential that produces bistability. To get faithful topographic images, working conditions close to the attractive-repulsive transition should be avoided.

Tapping-mode experiments are usually performed in air. It is a common experience that electrostatic charges may be accumulated on the surface of insulating materials. These electrostatic charges may produce large, unwanted attractive forces that may control the operation of the instrument with independence of the properties of the sample. In general, those situations should be avoided to obtain a good topographic tapping-mode image. Those forces have not been considered here.

The slope of the amplitude curve ($A_0 = 10$ nm) for intermediate or stiff materials in the attractive and repulsive regimes is unity [Fig. 2(a)]. The feedback mechanism will produce topographic images of the same quality irrespective of the operating regime. However, this may not apply when imaging very compliant samples. Those cases will be discussed elsewhere.[31]

We have found a large amount of experimental evidence that supports the conclusions of these calculations. For instance, discontinuities in the amplitude curves have been described by Anczykowski *et al.*[13,32] and Kühle, Soerensen, and Bohr[16] on SiO_x samples, and Haugstad and Jones on polyvinyl alcohol films.[33] Furthermore, phase-shift curves taken on polypropylene[30] and gelatine[34] surfaces show evidence of a continuous transition. The hysteresis loop shown by the frequency response curves has also been observed experimentally.[35]

The model considered here is in some respects an over simplification. In particular, the tip-cantilever is considered as a single-mass model, thus neglecting any higher modes of vibration of the cantilever. It also does not include any internal degree of damping (viscosity) or tip-sample inelastic interactions. Despite all these simplifications, the model yields amplitude vs distance and amplitude vs frequency curves that reproduce the experimental features. This reinforces the validity of the model to describe tapping-mode operation and supports the results of the simulations for situations to be explored experimentally.

ACKNOWLEDGMENT

This work has been supported by the European Commission, BICEPS, BIO4-CT-2112.

*Electronic address: rgarcia@imm.cnm.csic.es

[1] Y. Martin, C. C. Williams, and H. K. Wickramasinghe, J. Appl. Phys. **61**, 4723 (1987).

[2] T. R. Albrecht, P. Grütter, D. Horne, and D. Rugar, J. Appl. Phys. **69**, 668 (1991).

[3] F. J. Giessibl, Science **267**, 68 (1995); Phys. Rev. B **56**, 16 010 (1997).

[4] M. Guggisberg, M. Bammerlin, R. Lüthi, Ch. Loppacher, F. Battiston, J. L. A. Baratoff, E. Meyer, and H.-J. Güntherodt, Appl. Phys. A: Mater. Sci. Process. **66**, S245 (1998).

[5] Q. Zhong, D. Imniss, K. Kjoller, and V. B. Elings, Surf. Sci. **290**, L688 (1993).

[6] R. Pérez, Y. Stich, M. Payne, and K. Terakura, Phys. Rev. B **58**, 10 835 (1998).

[7] J. Tamayo and R. García, Langmuir **12**, 4430 (1996).

[8] C. Bustamante and D. Keller, Phys. Today **48**(12), 33 (1995); E. Margeat, C. Le Grimelle, and C. A. Royer, Biophys. J. **75**, 2712 (1998).

[9] G. Bar, Y. Thomann, and M.-H. Whangbo, Langmuir **14**, 1219 (1998).

[10] R. García, M. Calleja, and F. Pérez-Murano, Appl. Phys. Lett. **72**, 2295 (1998).

[11] J. Chen, R. Workman, D. Sarid, and R. Höper, Nanotechnology **5**, 199 (1994).

[12] R. G. Winkler, J. P. Spatz, S. Sheiko, M. Möller, R. Reineker, and O. Marti, Phys. Rev. B **54**, 8908 (1996).

[13] B. Anczykowski, D. Krüger, and H. Fuchs, Phys. Rev. B **53**, 15 485 (1996).

[14] N. A. Burham, O. P. Behrend, F. Ouveley, G. Gremaud, P.-J. Gallo, D. Gordon, E. Dupas, A. J. Kulik, H. M. Pollock, and G. A. D. Briggs, Nanotechnology **8**, 67 (1997).

[15] S. John, T. Van Noort, Kees O. Van der Werf, Bart G. De Grooth, Niek F. Van Husl, and Jan Greve, Ultramicroscopy **69**, 117 (1997).

[16] A. Kühle, A. H. Soerensen, and J. Bohr, J. Appl. Phys. **81**, 6562 (1997).

[17] A. Bugacov, R. Resch, C. Baur, N. Montoya, K. Woronowicz, A. Papson, B. E. Koel, A. Requicha, and P. Will, Probe Microscopy (to be published); R. Resch, A. Bougacov, C. Baur, B. E. Koel, A. Madhukar, A. A. G. Requicha, and P. Will, Appl. Phys. A: Mater. Sci. Process. **67**, 265 (1998).

[18] D. Sarid, T. G. Rushell, R. K. Workman, and D. Chen, J. Vac. Sci. Technol. B **14**, 864 (1996).

[19] U. Rabe, J. Turner, and W. Arnold, Appl. Phys. A: Mater. Sci. Process. **66**, S277 (1998).

[20] G. Chen, R. Warmack, A. Huang, and T. Thundat, J. Appl. Phys. **78**, 1465 (1995).

[21] S. Ciraci, E. Tekman, A. Baratoff, and Y. P. Batra, Phys. Rev. B **46**, 10 411 (1992).

[22] J. Israelachvili, *Intermolecular and Surface Forces* (Academic, Orlando, 1991).

[23] B. V. Derjaguin, V. M. Muller, and Y. P. Toporov, J. Colloid Interface Sci. **53**, 314 (1975).

[24] L. D. Landau and E. M. Lifshitz, *Mechanics* (Pergamon, Oxford, 1960).
[25] J. M. T. Thompson and H. B. Stwart, *Nonlinear Dynamics and Chaos* (Wiley, New York, 1986).
[26] P. Gleyzes, P. K. Kuo, and A. C. Boccara, Appl. Phys. Lett. **58**, 2989 (1991).
[27] S. Fain (unpublished).
[28] A. P. French, *Vibrations and Waves* (Norton, New York, 1971).
[29] J. Tamayo and R. García, Appl. Phys. Lett. **73**, 2926 (1998).
[30] J. Tamayo and R. García, Appl. Phys. Lett. **71**, 2394 (1997).
[31] A. San Paulo and R. García (unpublished).
[32] B. Anczykowski, D. Krüger, K. L. Babcock, and H. Fuchs, Ultramicroscopy **66**, 251 (1996).
[33] G. Haugstad and R. Jones, Ultramicroscopy **76**, 77 (1999).
[34] X. Chen, M. C. Davies, C. J. Roberts, S. J. B. Tendler, P. M. Williams, J. Davies, A. C. Dawkes, and J. C. Edwards, Ultramicroscopy **75**, 171 (1998).
[35] L. Wang, Appl. Phys. Lett. **73**, 3781 (1998).